

A model for concrete perforation based on the concept of drilling strength

M. Borri Brunetto, A. Carpinteri & B. Chiaia

Department of Structural Engineering, Politecnico di Torino, 10129 Torino, Italy

ABSTRACT: A model for core drilling in concrete is introduced through a kinematical constraint to the process (helical trajectories of the cutters). By coupling the kinematic condition with the mechanical balance of engine power and drilling energy, a global formulation is obtained. The concept of drilling strength S , i.e. the energy consumed to remove a unit volume of material, is introduced. The drilling strength depends on the fracture mechanisms in the material, and thus on the geometry and size of the cutters. The model comprises a set of parameters which can be determined according to experiments.

Keywords: core-drilling, perforation, size-effects

1 INTRODUCTION

Core drilling represents an important process in many fields of engineering, e.g. civil, geotechnical and mine engineering. For instance, the extraction of cores from concrete structures is an every-day operation. Drilling into concrete is usually carried out under wet conditions, i.e., a flushing liquid (usually water) is used with the aim of cooling the cutting parts of the tool (to decrease their brittleness and wear rate) and of removing fragments outside the hole. Application of dry drilling (where the chips are removed by an air jet) is currently restricted to soft brick masonry, where temperatures at the cutting edges do not normally exceed 150-200 °C.

The demand for innovative tools able to drill into materials like reinforced concrete and hard rocks is increasing. However, research in the field has been limited, especially when compared to the wide literature concerning classical drilling tools for energy resources supply (Kerr, 1998). Extending results from these fields to the process of core drilling into concrete and masonry must be done with much care, since the ploughing action of the indenters is remarkably different from a traditional compressive action on soils and rocks. Neither can the theories of metal cutting be adopted in the presence of quasi-brittle materials, since plastic collapse is substituted by discontinuous chipping, fracture and fragmentation (Chiaia, 2001).

Two families of cutters for core drilling are available in the market, impregnated segments or single hard indenters. Impregnated segments (Miller & Ball, 1990, 1991) consist of a metal matrix where a distribution of small hard particles (usually synthetic diamonds or WC-Co particles) is embedded. Single indenters (Sneddon & Hall, 1988) are made of a metal support with a ultra-hard coating at the cutting edge (hard metal composites or polycrystalline diamond, e.g. PCD). Although the mechanical process is the same at the scale of the tool, the cutting action and the wear effects in the two cases are remarkably different at the scale of the cutters. It will be shown that significant scale effects, due to fracture mechanics, affect the performances of the cutters.

2 THE MODEL BY WOJTANOWICZ & KURU

2.1 Assumptions of the model

Wojtanowicz & Kuru (1993) derived a simple model for rock perforation which can be adapted to core-drilling in concrete. The model is based on the static balance of the forces acting on a single cutter, assuming similarity between bit and cutter. Three equations constitute the mathematical model: torque, drilling rate and bit life. The equations comprise cutter geometry, rock properties and four empirical constants, used to match the model to a real drilling process.

As shown in Figure 1, the model is derived from the analysis of the forces active at each cutter, where a certain wearflat is assumed to be already formed. In the model, R is the radius of the core-bit, u is the cutter penetration in the base material, ϑ is the cutting angle, β is the back rake angle (assumed as negative in Figure 1), λ is the side rake angle, f_n and f_t are respectively the normal and tangential forces acting upon the indenter, f_c is the cutting force (orthogonal to the cutting area), f_w is the component of the normal force orthogonal to the wear flat, f_{fw} and f_{fc} are the frictional forces acting respectively on the wear flat area and on the cutting surface area. Bit life, drilling rate, and bit torque equations are deduced from the balance of forces for a cutter moving with a constant angular velocity $\dot{\varphi}$. The following assumptions are made:

a) the base material displays plastic behavior (i.e., the local normal force f_n upon each cutter does not depend on the penetration u). We will show that, neglecting the f_n vs. u dependence represents a strong limitation of the model.

b) there is perfect mechanical similitude between a single cutter and the bit. Thereby, experimental evidence claims for the following assumptions:

- the advancement δ per bit rotation is proportional to the normal force f_n acting on a single cutter with proportionality constant k_1 ;
- the volumetric wear of the cutter is proportional to the work of friction at the contact area, with proportionality constant k_2 . The frictional drag at the cutter side surface is negligible.
- the drilling rate $\dot{\delta}$ is proportional to the cutter penetration u with proportionality constant k_3 ;
- the bit torque M_t is proportional to the single cutter's torque with proportionality constant k_4 .

c) if the penetration is small, also the cutting angle ϑ is small and can be ignored in the static balance. This means that the cutter moves in the direction perpendicular to the stud axis. This assumption, which contradicts the evidence for helicoidal trajectories, does not affect the static balance.

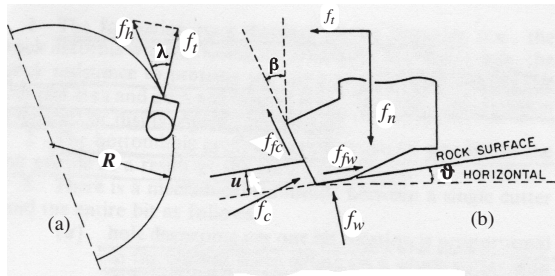


Figure 1. Static balance of the forces acting upon a cutter.

2.2 Balance equations

Under the above hypotheses, the equilibrium diagram of the forces active between the rock and the cutter can be easily obtained. For small values of the cutting depth, the effect of the cutting angle ϑ can be ignored. The normal and tangential components can be expressed according to the following equations:

$$f_n = f_c \sin \beta + f_{fc} \cos \beta + f_w \cos \vartheta + f_{fw} \sin \vartheta \quad (1-a)$$

$$f_t = f_c \cos \beta - f_{fc} \sin \beta + f_{fw} \cos \vartheta - f_w \sin \vartheta \quad (1-b)$$

We can put $f_c = S_c A_c$, $f_{fc} = \mu f_c = \mu S_c A_c$ and $f_{fw} = \mu f_w = \mu S_w A_w$, where μ is the sliding friction coefficient between cutter and base material, S_c and S_w are respectively the resistance to crushing and the resistance to penetration of the base material, A_c is the cutting area ($A_c = tu$), and A_w is the wear flat area. Assuming $\vartheta \approx 0$ one obtains:

$$f_n = S_c A_c (\sin \beta + \mu \cos \beta) + S_w A_w, \quad (2-a)$$

$$f_t = S_c A_c (\cos \beta - \mu \sin \beta) + \mu S_w A_w \cong f_h. \quad (2-b)$$

Notice that, as currently detected in drilling operations (Glowka, 1989), the penetrating force f_n imposed on a worn cutter at a given depth is nearly proportional to the wearflat area A_w in contact with the base material.

2.3 Drilling rate equation

The normal force balance equation can be solved for the cutting surface as:

$$A_c = \frac{f_n - S_w A_w}{S_c (\sin \beta + \mu \cos \beta)} \quad (3)$$

The cutting area, for a single cutter, is a function of the penetration and of the wear state. Wear was considered by the Authors through a dimensionless function U_D . Therefore, they obtained:

$$u = \frac{U_D (f_n - S_w A_w)}{t S_c (\sin \beta + \mu \cos \beta)}, \quad (4)$$

where t is the width of the cutter.

As the drilling velocity $\dot{\delta}$ is proportional to u through an empirical constant k_3 , if n_d is the number of cutters on the core bit, the bit progress per one full rotation is n_d -fold greater than u . Thus, the drilling

rate, according to Wojtanowicz & Kuru (1993), is given by:

$$\dot{\delta} = k_3(\dot{\varphi})^{k_5} n_d u \quad (5)$$

Inserting Eq. (4) into Eq. (5), we obtain:

$$\dot{\delta} = k_3(\dot{\varphi})^{k_5} \frac{U_D(F_n - F_0)}{tS_c(\sin\beta + \mu\cos\beta)} \quad (6)$$

where $F_n = n_d f_n$, $F_0 = n_d S_w A_w$, $\dot{\varphi}$ is the angular velocity of the bit and k_5 is an exponent accounting for possible nonlinearities due to inadequate bottomhole cleaning. According to this model, the drilling velocity is independent of n_d . We will see that the role of n_d does not come into play because of neglecting nonlinearity of the penetration law.

2.4 Bit torque equation: role of the rake angle β

Let us merge the balance equations (2a) and (2b). The horizontal force on each cutter reads as:

$$f_h = f_n \left(\frac{1 - \mu \tan\beta}{\mu + \tan\beta} \right) - S_w A_w \left(\frac{1 - 2\mu \tan\beta - \mu^2}{\mu + \tan\beta} \right) \quad (7)$$

and the total torque M_t is simply given by $M_t = n_d R f_h$. It can be deduced that, for constant normal thrust on the bit, the active torque becomes a unique decreasing function of the wearflat area.

It is known that, for negative rake angles, as the inclination is decreased, the cutting action becomes more efficient (Kerr, 1988). The drilling strength (e.g. the specific drilling energy, see Section 3.3) decreases for the same thrust on the bit. This makes the bit more aggressive and, all other things being equal, a higher drilling velocity is attained. The smaller rake angle, however, makes the cutter more vulnerable to impact breakage should a hard particle be encountered. Conversely, a cutter with a larger rake angle will produce smaller chips but will be more durable in hard concretes, providing longer bit life.

According to the model by Wojtanowicz & Kuru (1993), when all the other operational parameters are fixed, the drilling velocity is maximum for $\beta=0$. This would suggest to use rake angles as small as possible. In the real situations, a minimum value of the negative rake angle is convenient with respect to $\beta=0$, since it is usually accompanied by a finite value of the clearance angle γ .

On the other hand, the theories of metal cutting suggest that, for cutting rebars in reinforced concrete, positive rake angles are more efficient.

This is because a combined shear-bending action is provided, which favours continuous chip formation. Considering the balance equations (1), we notice that, for positive rake angles, the only variation is the sign of the $\sin\beta$ term. Thereby, all the other quantities being the same, the normal force f_n is smaller, while the horizontal force f_t is larger. This is a rather intuitive conclusion, although one has to remind that the assumptions of the model rely on a plastic rupture mechanism which is not very likely to occur in the presence of positive rake angles. In addition, a high wear rate can dramatically reduce the cutting ability of the indenters with positive back-rake angle.

3 HELICOIDAL MODEL FOR CORE DRILLING

3.1 Kinematic assumptions

The hypothesis of (circular) horizontal trajectories of the cutters, although acceptable at the level of force balance at the cutting edge, hinders important aspects of the core drilling process. In particular, it is impossible to model a continuous process. In order to model a continuous, stationary process and to respect the rotational symmetry (no cutter prevails over the others), it is necessary to consider intersecting helicoidal trajectories. Each cutter is subjected to a normal component f_n (due to the penetration) and to a tangential one f_t (the cutting force) due to the ploughing action. Given two cutters D1 and D2 in a core bit with radius R , at a distance $s=2\pi R/2$ (Fig. 2), the torsion of the helix provides the angle ϑ (the cutting angle), which can be considered as a measure of the rate of advancement (i.e., of the drilling velocity $\dot{\delta}$).

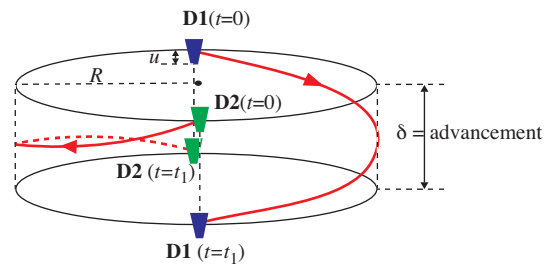


Figure 2. Helicoidal trajectories of the cutters.

We can generalize the process to an arbitrary number n_d of cutters, equally spaced within the circumference with radius R . Their mutual distance s will thus be:

$$s = \frac{2\pi R}{n_d} \quad (8)$$

Let us suppose that the penetration u is the same for all the cutters. This assumption is quite reasonable in a stationary regime, due to progressive wear of the indenters. One can immediately notice that, for a generic value of δ , each cutter, when reaching the position previously occupied by the cutter in front of it (i.e., after a rotation equal to $2\pi/n_d$), must face an obstacle of height δ . In particular, two situations may occur.

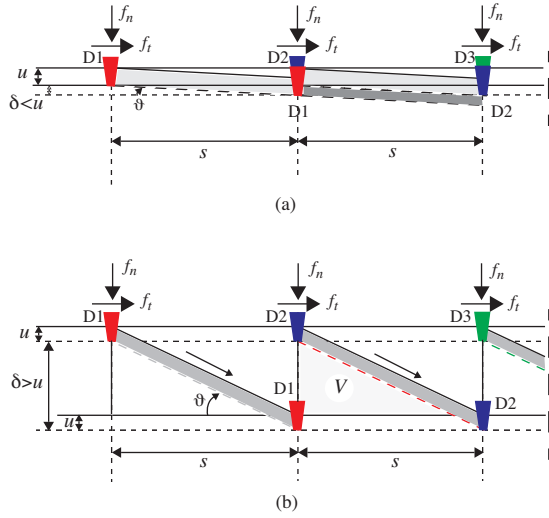


Figure 3. Non stationary drilling situations. Decreasing (a), and increasing (b) drilling velocity.

If $\delta < u$, each cutter would experience a decrease of its penetration (e.g. $u \rightarrow \delta$, decreasing normal thrust) whereas, if $\delta > u$, each cutter would face an obstacle of height larger than its penetration and this would imply an increase of its penetration (e.g. $u \rightarrow \delta$), which is possible only under the increase of the normal force. Both situations refer to non-stationary drilling (Fig. 3).

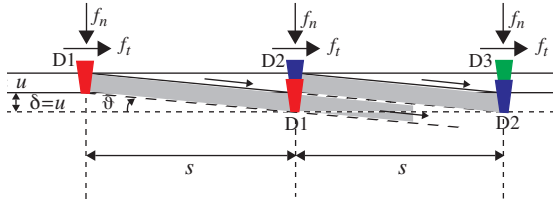


Figure 4. Optimal kinematic condition for the cutters.

Thus, the optimal value $\bar{\theta}$ corresponds to the condition $\delta = u$, or, in other words, each cutter must continuously face an obstacle of height exactly

equal to its penetration (Fig. 4). The optimal value of the cutting angle must be directly related to the penetration and to the mutual distance among the cutters:

$$\tan(\bar{\theta}) = \frac{u}{s} \quad (9)$$

The apparently strange conclusion is that *the rate of advancement $\bar{\theta}$ depends on the base material only by means of the penetration u* . The helicoidal advancement is controlled by kinematic quantities. The smaller the separation distance (in the direction of the motion) among the cutters (i.e. the larger n_d), the larger must be the advancement, for a given penetration, to ensure a stationary efficient process. Note, incidentally, that a larger number of active cutters requires a larger thrust on bit (and thus a larger value of the active torque M_t) to keep a certain value of the penetration u .

3.2 Kinematic determination of the drilling velocity

If $\dot{\varphi}$ is the angular velocity of the core bit, the tangential velocity of the cutters is equal to $\dot{\varphi}R$. Thus, the drilling velocity is given by:

$$\dot{\delta} = \tan(\bar{\theta})\dot{\varphi}R = \frac{u}{s}\dot{\varphi}R = un_d\frac{\dot{\varphi}}{2\pi} \quad (10)$$

where we have used Eqs. (8) and (9). Notice the remarkable similarity between Eq. (5) and Eq. (10) obtained by Wojtanowicz & Kuru (1993) by means of empirical assumptions. The optimal rate of advancement $\bar{\theta}$ depends on the base material by means of the indenters penetration u . Consider the following general penetration law for a single indenter:

$$f_n = ku^\alpha \quad (11)$$

where f_n is the normal force upon the indenter, and k , α are two constants depending on the base material, the indenter geometry and the wear state.

As is well known in mechanics, the value $\alpha \approx 2$ is valid for elasto-plastic indentation of cones and pyramids. It can be used for each small indenter embedded into a impregnated segment, but is not valid for the penetration of the whole cutter since the total contact area is not constant. In the presence of large, single hard indenters, the situation is closer to a 2D wedge with a linear load-penetration law in the elastic regime (Fisher Cripps, 2000).

Regarding the base material, we may argue that exponents larger than 1.0 should be used for a very

hard base material whereas, when compressive failure of the base material is governed by plasticity, values of $\alpha \leq 1$ become more reliable. Simulations by the lattice model (Fig. 5) have shown that α can be lower than 1.0 if heterogeneity and cumulative damage of the base material are considered (Carpinteri et al., 2003). This would explain why, in some cases (usually related to high thrust or to very soft materials), the rate of increase of $\dot{\delta}$ with F_n is more than linear (see Equation (13)). In any case, the value $\alpha=1$ corresponds to the experimentally detected almost linear dependence of $\dot{\delta}$ on F_n .

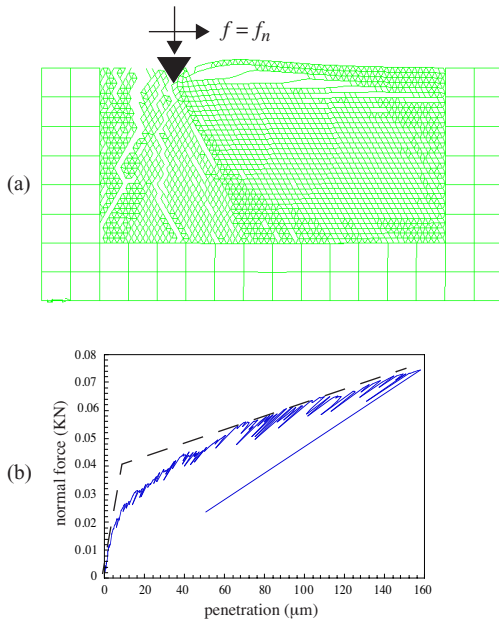


Figure 5. Lattice simulation of the cutting process (a); load-penetration response (b).

One should also take into account that the development of wear flats (with drilled distance) provides the progressive increase of the penetration stiffness k . Assuming that $F_n = n_d f_n$, one easily obtains:

$$u = \frac{F_n^{1/\alpha}}{(n_d k)^{1/\alpha}} \quad (12)$$

Inserting the above relation into eq. (10), one gets:

$$\dot{\delta} = \frac{F_n^{1/\alpha} (n_d)^{(1-1/\alpha)} \dot{\varphi}}{2\pi k^{1/\alpha}} \quad (13)$$

which represents the optimal kinematic functioning point of core drilling.

Equation (13) implies that, if the drilling process is carried out at constant angular velocity, the drilling strength does not influence the drilling velocity provided there is always sufficient supply of mechanical energy. The drilling velocity, except for the case when $\alpha=1$, is also depending on the number n_d of active indenters. In particular, in the case $\alpha < 1$ (disordered soft materials, crushing failure), the exponent of n_d in Eq. (13) becomes negative, and thus a smaller number of indenters implies a larger drilling velocity. On the contrary, when $\alpha > 1$ (hard homogeneous materials, brittle chipping), the exponent is positive and therefore a larger number of cutters provides better performances.

3.3 Definition of the drilling strength S

Electrical engines can balance larger torques, at fixed angular velocity, by increasing the mechanical power supplied to the bit. The characteristic curves of the engine permit to obtain the dependence of the quantity P_{mech}/M_t on the angular velocity $\dot{\varphi}$.

In order to define a mechanical functioning point, we need to balance the work provided by the engine with the work dissipated by removing the base material through the cutting action. The core drilling process in quasi-brittle materials like concrete and masonry involves different sources of energy expenditure. In particular, frictional energy dissipation with considerable heat production occurs and secondary processes like fragmentation and milling also add to the basic fracture process and contribute to the total amount of dissipated energy. The precise determination of each contribution is awkward since it depends on the geometrical characteristics of the cutter, on the activated friction, on the flushing liquid and also on the operating conditions. Therefore, the simplest way to proceed is to collect all the sources of energy expenditure into a single quantity, called the “drilling strength” S , defined as the specific energy required to remove the unit volume of the base material during a certain drilling process.

According to this global definition, the drilling strength is measured as Joule/m³ or N/m², and therefore S has the same physical dimensions of material strength σ_u and Young’s modulus E . As a first approximation, in fact, the drilling strength S of a certain material can be considered as proportional to its ultimate (crushing) stress σ_u . However, since the drilling strength S depends on the size and shape of the indenters, it is not a material constant but undergoes remarkable size effects (see Section 4).

As shown in Figure 6, the drilling strength can be related to the cutting force f_t . By equating the work done by the cutting force f_t to the work dissipated by

crushing during an horizontal advancement v of the cutter, one obtains the cutting force simply as:

$$f_t = S(ut) \quad (14)$$

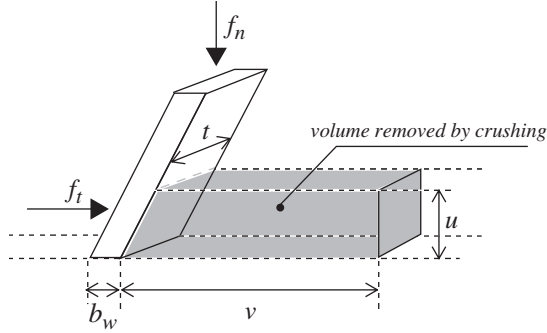


Figure 6. Simple crushing model for the definition of the drilling strength S .

Another global quantity that can be used as a measure of energy expenditure is the pseudo-friction coefficient $\mu^* = F_t/F_n$. The drilling strength can be related to μ^* by simple balance arguments. The mechanical power provided by the engine can be expressed, in fact, by means of the active torque, as a linear function of μ^* or as a linear function of S :

$$W = M_t \dot{\varphi} = \mu^* F_n R \dot{\varphi} = S A_{bit} \dot{\delta} \quad (15)$$

where $A_{bit} = 2\pi R t$ represents the circular projected area of the groove (t represents the width of the groove made by the cutters). Comparing the two formulations, one obtains:

$$\mu^* = \frac{S t}{k} \quad (16)$$

i.e. the pseudo-friction coefficient can be expressed as a function of the drilling strength and of the penetration stiffness. Equation (16) permits to relate the general kinematic model of drilling to the simpler Coulomb approach, based on the pseudo-friction coefficient $\mu^* = F_t/F_n$ (Davim et al., 2000).

Having defined the drilling strength S , we can now couple the kinematic description of the drilling process with the mechanical balance equation. By equating the externally supplied mechanical power P_{mech} to the power dissipated by crushing the base material, one obtains the mechanical functioning point :

$$\dot{\delta} = \frac{\eta P_{mech}}{S 2\pi R t}, \quad (17)$$

where η represents the mechanical efficiency of the engine.

By equating Eqs. (13) and (17), the coupled equation of core drilling is obtained, where the kinematic and mechanical conditions are merged:

$$\frac{F_n^{1/\alpha} (n_d)^{(1-1/\alpha)} \dot{\varphi}}{2\pi k^{1/\alpha}} = \frac{\eta P_{mech}}{S 2\pi R t} = \dot{\delta} \quad (18)$$

The above equation can be specialised for different base materials and for different wear states. If the characteristic curve of the engine is known, all the regimes of drilling can be described. For instance, the maximum normal thrust (corresponding to the clogging limit) can be computed as a function of the maximum mechanical power:

$$(F_n)_{max} = k \left(\frac{\eta P_{mech}^{max}}{S R t (n_d)^{(1-1/\alpha)} \dot{\varphi}} \right)^\alpha \quad (19)$$

Also, the drilling strength corresponding to a certain drilling process can be calculated *a posteriori* from the experimental tests as:

$$S = \frac{\eta P_{mech} k^{1/\alpha}}{F_n^{1/\alpha} (n_d)^{(1-1/\alpha)} \dot{\varphi} R t} \quad (20)$$

The above equation confirms that, when $\alpha < 1$, if the minimum drilling strength is pursued, the number of cutters must be the smallest as possible. The opposite conclusion applies for $\alpha > 1$. In addition, it shows also that, all the other parameters being fixed, a larger thrust implies a smaller specific consumption of energy, according to several experimental tests (Miller & Ball, 1990, 1991).

4 SIZE EFFECTS ON DRILLING STRENGTH

The cutting force has been related to the drilling strength S by means of Equation (14). This simple approach permits to consider all the sources of energy dissipation occurring in the drilling process by means of a single mechanical quantity. More refined studies, at the level of the indenters, should permit to estimate the value of S on the basis of theoretical arguments. In the context of Strength of Materials, the physical dimensions of the drilling strength ($[F][L]^{-2}$) correspond to the assumption of crushing (plastic) collapse ahead of the cutter (see Figure 6).

When brittle fracture rather than plastic crushing dominates material collapse, a more consistent material parameter can be used, namely the fracture toughness K_{IC} , with the anomalous physical dimensions ($K_{IC}=[F][L]^{-3/2}$). Dimensional Analysis, in this case, provides:

$$f_t = K_{IC} \rho t u^{1/2} \quad (21)$$

where ρ is a nondimensional shape factor. Rearranging equation (18), we obtain the following alternative expression of the drilling velocity:

$$\dot{\delta} = \left[\frac{F_n}{k} \right]^{2\alpha} (n_d)^{-1/\alpha} \frac{P_{mech}}{2\pi R K_{IC} \rho t} \quad (22)$$

It can be noticed that the dependence of $\dot{\delta}$ on the normal force F_n is weaker than in the case of plastic collapse.

The above description, based on Fracture Mechanics, permits also to give theoretical basis to the measured size-effects on cutting strength, as already pointed out in a previous paper by Chiaia (2001). Let us consider two different indenters, pushed inside the base material by different values of the normal force (Fig. 7).

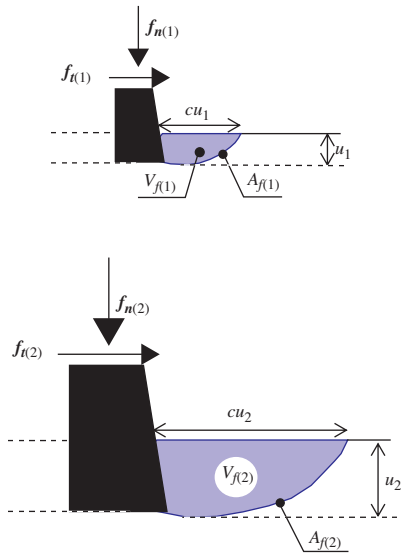


Figure 7. Geometrical similarity in the chipping problem.

Of course, two different values of the cutting force f_t are induced by the two situations. It is physically plausible to assert that self-similarity holds in the distribution of the fragments removed

by the ploughing indenters. Similitude is supported by the power-law distributions of the fragments obtained in drilling experiments (Turcotte, 1989). Thereby, assuming the penetration u as the reference length scale, the volume V_f of the removed chip scales as u^3 , while the area of the fracture surface A_f scales as u^2 .

The drilling strength S has been introduced in the model as a scale-independent parameter. Indeed, when the chipping process is discontinuous, the failure criterion must be written in terms of the stress-intensity factor K_I , to be compared with the fracture toughness of the material, K_{IC} . Thus, the cutting force f_t has to obey the following relation:

$$K_I = \frac{f_t}{\chi u^{3/2}} f(x, y, z) = K_{IC} \quad (23)$$

where χ is a nondimensional geometrical factor and $f(x, y, z)$ is a nondimensional geometrical function. Dimensional Analysis yields, in this case, the following scale dependence of the cutting force on the penetration: $f_t \sim u^{3/2}$. The above scaling law can also be justified by the dimensional disparity inherent to the energy balance. The elastic strain energy stored in the fragment, in fact, scales as u^3 , whereas the energy which can be dissipated along the fracture surface scales as u^2 . In the case of plastic crushing, instead, both energies would scale as u^3 .

The intrinsic nonlinearity of chipping (which is independent of the penetration law) implies that a Coulomb-like linear relation is misleading. In fact, in typical drilling experiments (see Mishnaevsky, 1994, 1995), the ratio f_t/f_n increases with u . Due to geometrical self-similarity of chips, one can assert that the work W done by the cutting force when removing a single fragment is given by the product of the force times a displacement cu (Fig. 7). Therefore, recalling eq. (14), we get:

$$W = (f_t \times cu) \sim u^{5/2} \quad (24)$$

where c is a nondimensional geometrical factor. From Eqs. (15) and (24) one obtains the following scaling law for the drilling strength:

$$S = \frac{W}{\kappa u^3} \sim \frac{1}{\sqrt{u}} \quad (25)$$

where κ is a nondimensional geometrical factor (see Figure 8).

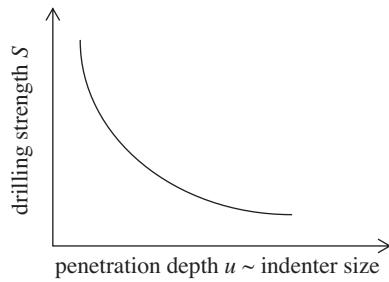


Figure 8. Size effects on the drilling strength.

The above scaling law is confirmed by the experiments. Single-scratch tests carried on large PCD cutters ($t=4\text{mm}$), have shown that the drilling strength is one order of magnitude larger than the material's compressive strength (e.g., $S=400\text{MPa}$ for a reference concrete). In the case of impregnated segments, instead, where the size of the indenting diamonds is much smaller ($t=100\mu\text{m}$) the measured drilling strength is close to 1000MPa . As expected, larger indenters activate less specific strength, i.e. they are more efficient although a larger normal force will be necessary to ensure their penetration. The square root scaling is modified in the presence of soft materials, because a certain extent of crushing always occurs immediately ahead of the indenter, and thus the two destruction mechanisms interact with each other (Van Kesteren, 1995).

5 GLOBAL EQUATION OF CORE DRILLING

The dependence of the drilling strength S on the back-rake angle can be expressed by relating the helicoidal theory of core drilling to the geometrical configuration of the single cutter. This dependence is explicitly taken into account by the static balance proposed by Wojtanowicz & Kuru (1993), although, in that theory, the cutting mechanism is restricted, whatever the back-rake angle, to plastic crushing.

Considering the balance equations (1), and expressing the drilling strength S as the work of the cutting force per unit of removed volume along the scratch, we obtain an expression where S can be related to a reference drilling strength S^* measured for $\beta=0$:

$$S(\beta) = S^* \frac{(\sin\beta + \mu \cos\beta)}{\mu} \quad (26)$$

The trigonometric term $(\sin\beta + \mu \cos\beta)$ is already present in the model by Wojtanowicz & Kuru (1993). Notice that, in the above model, positive

angles correspond to $\beta < 0$. Therefore, positive rake angles imply a lower apparent drilling strength, i.e., a better drillability. By inserting Eq. (26) in Eq. (18), one obtains the global equation of core drilling:

$$\frac{F_n^{1/\alpha} (n_d)^{(1-1/\alpha)} \dot{\phi}}{2\pi k^{1/\alpha}} = \frac{\eta P_{mech}}{S^* \frac{(\sin\beta + \mu \cos\beta)}{\mu} 2\pi R t} \quad (27)$$

which, in principle, permits to model any kind of drilling process. In order to consider in the model also cutter's wear, the dependence of the stiffness on the total drilled distance should be considered. This is a coupled problem, since the wear rate is affected by the relative hardness of the cutter and base material.

REFERENCES

- Carpinteri, A., Chiaia, B. and Invernizzi, S. 2003. Influence of material microstructure on the fracture induced by a hard cutting indenter. *Engineering Fracture Mechanics*, in print.
- Chiaia, B. 2001. Fracture mechanisms induced in a brittle material by a hard cutting indenter. *International Journal of Solids and Structures* 38: 7747-7768.
- Davim, J.P. and Monterio Baptista A. 2000. Relationship between cutting force and cutting tool wear in machining silicon carbide reinforced aluminum. *Journal of Material Processing Technology* 103: 417-423.
- Fischer-Cripps, A.C. 2000. *Introduction to Contact Mechanics*. Springer, New York.
- Glowka, D.A. 1989. Use of single-cutter data in the analysis of PDC bit design: Part 1- development of a PDC cutting force model. *Journal of Petroleum Technology*, August: 797-849.
- Kerr, C.J. 1988. PCD drill bit design and field application evolution. *Journal of Petroleum Technology*, March: 327-332.
- Miller, D. & Ball, A. 1990. Rock drilling with impregnated diamond microbits - an experimental study. *Int. J. Rock Mech. Min. Sci.* 27: 363-371.
- Miller, D. & Ball, A. 1991. The wear of diamonds in impregnated diamond bit drilling. *Wear* 141: 311-320.
- Mishnaevsky, L.L. 1994. Investigation of the cutting of brittle materials. *Int. J. Mach. Tools Manuf.* 34 : 499-505.
- Mishnaevsky, L.L. 1995. Physical mechanisms of hard rock fragmentation under mechanical loading: a review. *Int. J. Rock Mech. Min. Sci.* 32: 763-766.
- Sneddon, M.V. and Hall, D.R. 1988. Polycrystalline diamond: manufacture, wear mechanisms, and implications for bit design. *Journal of Petroleum Technology*, December: 1593-1601.
- Turcotte, D. 1989. Fractals in geology and geophysics. *Pure and Applied Geophysics* 131: 171-196.
- Van Kesteren, A. 1995. Numerical simulations of crack bifurcation in the chip forming cutting process in rock. In G. Balcer and B.L. Karihaloo (eds.), *Fracture of Brittle Disordered Materials*, E & FN Spon, London: 505-524.
- Wojtanowicz, A.K. and Kuru, E. 1993. Mathematical modelling of PDC bit drilling process based on single cutter mechanics. *ASME Journal of Energy Resources Technology* 115: 247-256.